IL NUOVO CIMENTO Vol. 26 C, N. 2 Marzo-Aprile 2003

# Cosmic-ray transparency for a medium-latitude observatory

P. Bobik([1]), M. Storini([2]), K. Kudela([1]) and E. G. Cordaro([3])

([1]) *IEP/SAV - Watson str. 47, 004353 Košice, Slovak Republic*
([2]) *IFSI/CNR - Via del Fosso del Cavaliere 100, 00133 Roma, Italy*
([3]) *Department of Physics/FCFM, UChile - P.O. Box 487-3, Santiago, Chile*

(ricevuto il 18 Novembre 2002; approvato l'11 Aprile 2003)

**Summary.** — The access of cosmic-ray particles to a medium-latitude observatory is analysed from results coming from the numerical solution of the charged-particle motion in the geomagnetic field. Evaluations are performed mainly for the Lomnický Štít neutron monitor location (LS: 2634 m a.s.l., geographic coordinates 49.20° N, 20.22° E), but some results for the Antarctic Laboratory for Cosmic Rays (LARC: 40 m a.s.l, 62.20° S and 301.04° E) are also given. Particular attention is paid to the variability of the magnetospheric screening appearing when the external magnetic field is added to the internal one.

PACS 96.40.-z – Cosmic rays.
PACS 93.30.Ge – Europe.
PACS 93.30.Ca – Antarctica.

## 1. – Introduction

Cosmic-ray (CR) trajectory computations are the usual tool to evaluate the magnetospheric screening effect for arriving charged particles on the Earth ground. To this end, there exist several computational codes for particle tracing in a given geomagnetic-field model (*e.g.* [1-6], among others). Recently Shea *et al.* [7] reviewed the subject. All these codes are based on the numerical solution of the equation of motion for charged particles in a selected model of the geomagnetic field. Here we discuss a method based on the Runge-Kutta (RK) 6th-order approximation of the above equation (sect. **2**). The influence of the geomagnetic activity level on the penumbra structure (sect. **3**), on the asymptotic directions of the vertically incident particles (sect. **4**), as well as on their oblique directions (sect. **5**), are described for a cosmic-ray observatory located at a medium geomagnetic latitude (*i.e.* included in the 30°–60° geomagnetic latitudinal range). Also possible effects affecting the cosmic-ray penumbra induced by energy losses during complicated particle trajectories in the residual atmosphere are discussed (sect. **6**). Evaluations are performed mainly for the Lomnický Štít neutron monitor location (LS: 2634 m a.s.l., geographic coordinates 49.20° N, 20.22° E), but some results for the Antarctic

 

Laboratory for Cosmic Rays (LARC: 40 m a.s.l, 62.20° S and 301.04° E; [8, 9]) are also given.

## 2. – Our trajectory computation method

For the accessing particles to a detector (position: $x, y, z$), the sign of the particle charge, as its velocity vector, is inverted; the trajectory is numerically traced with the initial conditions $(x, y, z, v_x, v_y, v_z)$ in the field model $\mathbf{B}(x, y, z)$ to obtain the solution of the equation

$$m \cdot \mathrm{d}\mathbf{v}/\mathrm{d}t = Z \cdot q \cdot [\mathbf{v} \times \mathbf{B}]\,, \tag{1}$$

where $m, q, Z, \mathbf{v}, \mathbf{B}$ are the relativistic mass, elementary charge, particle charge in elementary charge units, velocity and magnetic-field induction, respectively. For the simplest case of a homogeneous static magnetic field the gyroradius is

$$G_R = (m \cdot v)/(Z \cdot q \cdot B)\,. \tag{2}$$

For the solution of the differential equation system the Runge-Kutta method of 6th-order (RK6) approximation was used. The elementary step (namely the $n$ value) is defined in the following way: within its elementary step the trajectory is approximated as a straight line along the length interval: $\Delta l = G_R \cdot 2\pi/n$, or during the time interval: $\Delta t = 2\pi \cdot m/(Z \cdot q \cdot B \cdot n)$ and the new position values $(x_n, y_n, z_n, v_{xn}, v_{yn}, v_{zn})$ are found. In the next step the new point is adjusted as the initial one, and the same procedure is repeated from that point with the new velocity. For a description of the initial code, and a comparison of RK4 and RK6 methods (pointing to advantages of RK6 use), see [10].

Since the geomagnetic field is inhomogeneous and the $n$ value is derived from the initial point, another restriction was put into the computations: at each new point the angle $(\alpha)$ between the initial and new vector $\mathbf{v}$ is measured and compared with a limit value that we will call $\epsilon$. When $\alpha < \epsilon$, the elementary step is taken as a half of that adjusted according to the local field value at the initial point and the procedure is repeated from the begining. The $\epsilon$ value was taken as 0.01 rad and $n = 100$. Another parameter of our computations is the limiting number of elementary steps $(N)$ considered for each one of the trajectories (see below). Finally, the computation is ended in any one of the three cases:

i) the particle is crossing the Earth's surface (*forbidden trajectory*),

ii) the particle is crossing the magnetospheric boundary (*allowed trajectory*), or

iii) after $N$ steps neither decision of allowed or forbidden trajectory is obtained.

During the particle trajectory computations the conservation of $v$ (velocity module) is checked by $\eta = |(v_{\mathrm{initial}} - v_{\mathrm{current}})/v_{\mathrm{initial}}| < \delta$, being usually $\delta = 10^{-4}$. If $\eta$ is larger (seldom case), the computation is stopped for this trajectory and the computation procedure is repeated with refined parameters. The boundary condition for ii) is either the magnetopause crossing on the dayside (using the analytical model of Sibeck *et al.* [11]), or 25 Re (Re: Earth radius) sphere crossing on the nightside magnetosphere. Since near the magnetopause the field is relatively weak and the elementary step rather high, a refinement near the border (shortening the step) is applied to cross the model border at a distance less than 0.002 Re. At this point the asymptotic directions according to

TABLE I. – *LARC location (*62.20° *S and* 301.04° *E): $R_{\rm L}$, $R_{\rm U}$, and $R_{\rm C}$ for different $N$ values and* 1995 *epoch.*

| cut-off/$N$ | 5000 | 25000 | 100000 | 500000 | Ref. [22] |
|---|---|---|---|---|---|
| $R_{\rm L}$ | 2.927 | 2.671 | 2.290 | 1.891 | 2.57 |
| $R_{\rm U}$ | 3.215 | 3.208 | 3.208 | 3.208 | 3.21 |
| $R_{\rm C}$ | 3.136 | 2.972 | 2.890 | 2.881 | 2.97 |

the concepts reported by Shea and Smart [2, 3] are obtained (see [12], for a detailed description of the cut-off terminology).

The initial value of the velocity module is taken from the particle rigidity ($R$) which is stepwise. Hence, trajectory calculations are initiated at a rigidity value well below the expected cut-off, and continue at discrete intervals ($S$) of rigidity. We used $S = 0.001$ GV till rigidity values above which no forbidden trajectories exist.

In the following we denote $R_{\rm L}$, $R_{\rm U}$, and $R_{\rm C}$ as lower, upper and effective cut-off rigidities [12]. They are the first (in the order of increasing rigidity) forbidden/allowed transition, the last allowed/forbidden transition, and $R_{\rm C} = R_{\rm U} - \Sigma\Delta R_{\rm i}$, where $\Delta R_i$ are allowed trajectory intervals between $R_{\rm L}$ and $R_{\rm U}$.

The distribution of the magnetic field $\mathbf{B}(x, y, z)$ is given by the gradient of the scalar magnetic field potential being a sum of two terms: 1) related to the currents within the core (*internal field*) and 2) connected to the magnetosphere (*external field*, *i.e.* flowing on the magnetopause, within the tail and within the ionosphere). The three components of the resulting field vector are obtained as partial derivatives of the total potential [13].

The internal magnetic field is adjusted by IAGA in the form of Gauss coefficients of the spherical harmonic expansion of the potential up to the 10th order and with the epoch time step of 5 years. IGRF (International Geomagnetic Reference Field) and consequently DGRF (Definitive Geomagnetic Reference Field) are commonly used for the approximation of the internal field. Its main variability, which is of a long-term character, is due to secular effects of the internal current systems [14].

The external field is approximating the short-term variations of the magnetospheric current systems and introducing the local time asymmetry of the magnetosphere. Here we use the Tsyganenko 89 model (Tsyg89 [15]), which is giving the spatial distribution of $\mathbf{B}$ by using the geomagnetic $Kp$ index as a parameter (see [16-18], for a more detailed description of the external field model and [19-21], among others, for early studies on cut-off changes during magnetospheric disturbances).

Finally, we notice that, particularly for the rigidity penumbra ($P = R_{\rm U} - R_{\rm L}$) region, the number of steps ($N$) selected in the trajectory computation is a relevant parameter. Its adjustement gives also information on the consistency of the obtained results with those coming from other methods of computations. While for high rigidities (*i.e.* not complicated particle trajectories) $N$ is not a critical parameter and even $N = 5000$ gives a sufficient accuracy, for a medium-latitude geomagnetic observatory (characterised by a large rigidity penumbra) it is not the case. As an example, we report in table I the values of $R_{\rm L}$, $R_{\rm U}$, and $R_{\rm C}$, obtained with different $N$ values for LARC, assuming the vertical direction for the particle arrival and the IGRF model for epoch 1995. The last column reports values obtained by another evaluating method applied by Storini *et al.* [22].

The upper and effective cut-off rigidities are relatively stable and we notice a slightly decrease with the $N$ increase. It arises because with the $N$ increase a part of the computed

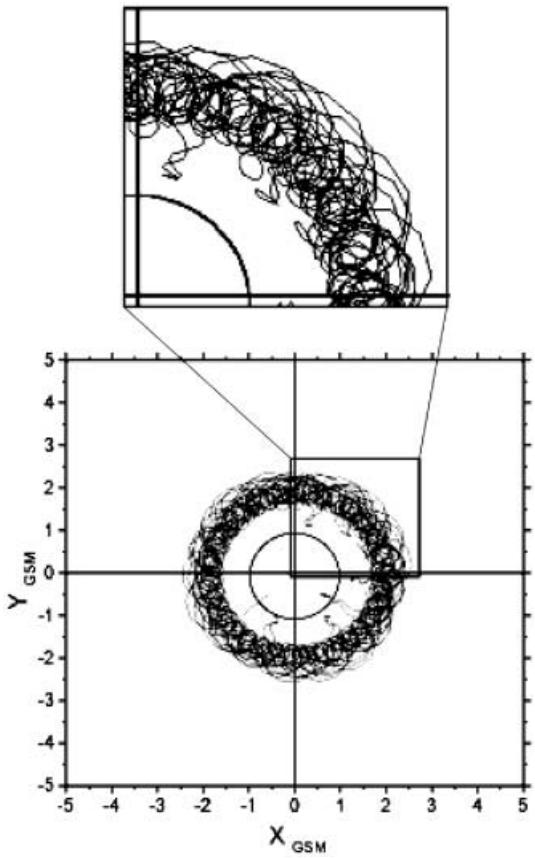


Fig. 1. – The projection of a particle trajectory of 2.25 GV rigidity computed for the vertical direction at LS position (49.20° N, 20.22° E) to $XY$ (GSM coordinates; unit: 1 Earth radius) plane and a zoom of a part (top pannel). The total length of the trajectory was $3.5 \times 10^6$ km before its stopping ($N = 250000$), corresponding to 12.6 s time-history of the tracing.

trajectories originally adjusted as iii)-category becomes of ii)-category. Instead, the lower cut-off is systematically and strongly decreasing with $N$. This effect should be related to the small rigidity step used by us in the penumbra region (*i.e.* 0.001, to compare with 0.01 applied by [22]). It seems that the refinement of the rigidity step and the $N$ increase lead to a strong decrease of $R_{\mathrm{L}}$.

Using the above comparison we adjusted in most of the computations listed below $N = 25000$ which, at least for $R_{\mathrm{U}}$ and $R_{\mathrm{C}}$, gives from one side a good consistency with another independent evaluating method, from another side it is not drastically increasing the computing time consumptions. There are however cases of complicated trajectories at medium latitudes which, even after 250000 steps, remains to be unresolved (quasi-trapped particles). Figure 1 exemplifies the trajectory for a 2.25 GV charged particle.

TABLE II. – *Results for LS location (49.20° N, 20.22° E) using DGRF models and the corresponding local L value for five different epochs.*

| Value/Epoch | 1965 | 1970 | 1975 | 1980 | 1985 | 1990 |
|---|---|---|---|---|---|---|
| $R_{\mathrm{L}}$ | 3.634 | 3.636 | 3.642 | 3.624 | 3.599 | 3.498 |
| $R_{\mathrm{C}}$ | 4.044 | 4.047 | 4.054 | 4.033 | 3.994 | 3.883 |
| $R_{\mathrm{U}}$ | 4.172 | 4.178 | 4.184 | 4.160 | 4.117 | 4.005 |
| $L$ | 2.031 | 2.028 | 2.025 | 2.028 | 2.034 | 2.039 |

## 3. – More on the cosmic-ray penumbra

The region between $R_{\mathrm{L}}$ and $R_{\mathrm{U}}$ (the penumbra) is often complicated and its structure depends on the geomagnetic-field model used. Here we summarise results obtained for LS location, both from internal and external magnetic-field models.

Using only DGRF models, calculations with our code were done with a 5-year step (from 1965 to 1990) and compared with the local McIlwain ($L$) value [23] in these periods.

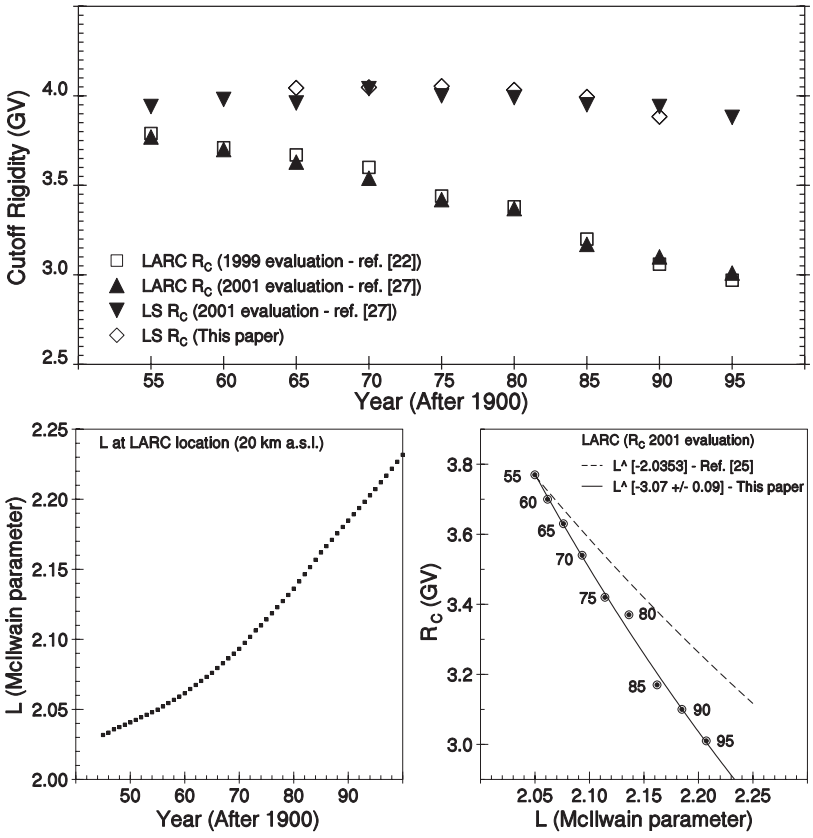


Fig. 2. – Long-term $L$ trend (lower left panel) for LARC (1945-2000), $R_{\mathrm{C}}$ for LARC *vs.* $L$ at 20 km (lower right panel) and comparison between different $R_{\mathrm{C}}$ evaluations (upper panel) for LARC and LS. See the text for details.

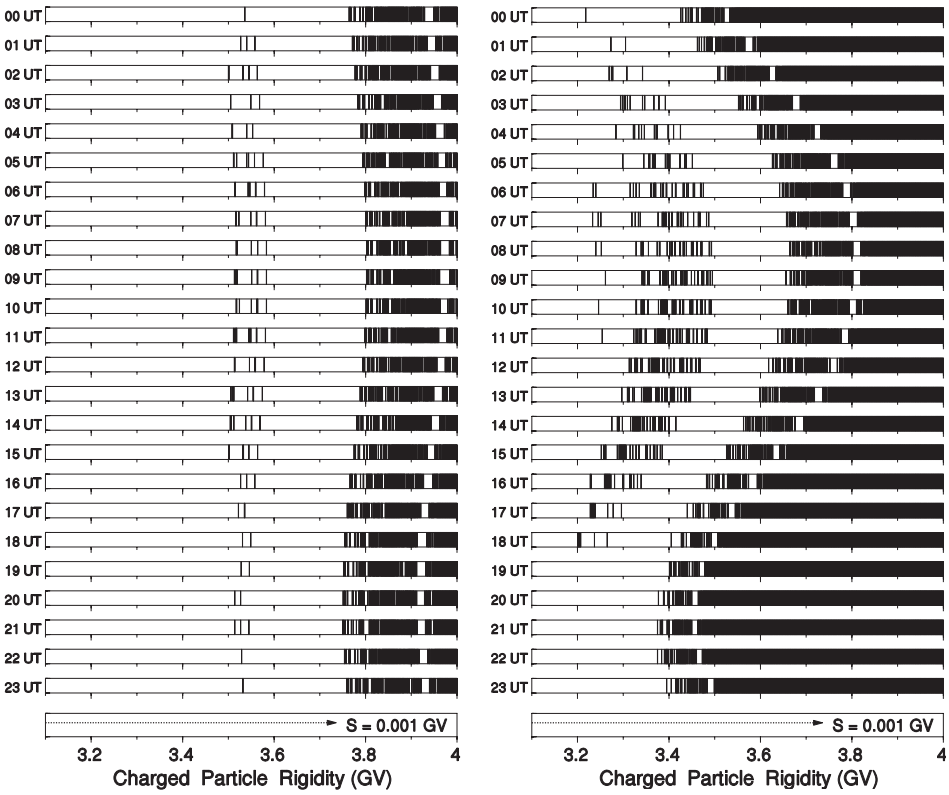


Fig. 3. – LS location (49.20° N, 20.22° E): allowed (black) and forbidden (white) particle rigidities evaluated with 1 h step for March 21, 1990 using Tsyg89 for the lowest ($Kp = 0, 0^+$; left panel) and highest ($Kp \geq 5^-$; right panel) levels of the geomagnetic activity. The rigidity interval 3.1–4.0 GV (for which $S = 0.001$ and $N = 25000$) is shown.

Results are shown in table II and reported as open diamonds in the upper panel of fig. 2. For the $L$ calculations a CADR code was used [24].

The long-term change of the local $L$ value at LS has a minimum around the 1975 year, which corresponds to the maximum cut-off at the effective, lower and upper rigidities. These results are consistent with past estimations of the $R_C$ and $R_U$ dependence on McIlwain's parameter, at least on a first approximation. In fact, for different periods, and based on data for many locations (epochs 1955, 1965 and 1980), it was derived that the three cut-off rigidities $R_L$, $R_C$ and $R_U$ follow a time dependence proportional to $L^{-\alpha}$, with $\alpha \sim 2$ [25]. However, the $L$ changes for LS are relatively small and the test of the proposed approximation is not very decisive [26]. Moreover, we performed more computations starting at three different altitudes: 20 km, 50 km and 100 km above the LS observatory. As expected, a systematical decrease of all the cut-offs, especially of the effective and upper rigidities, was obtained with the increasing altitude.

Returning to the long-term variability of cut-off rigidities, Shea and Smart [27] recently have computed vertical effective cut-off rigidities (from 1955 to 1995) for a long list of neutron monitor stations, using only the internal geomagnetic field described by IAGA coefficients. LS and LARC locations were considered; the new values are reported by

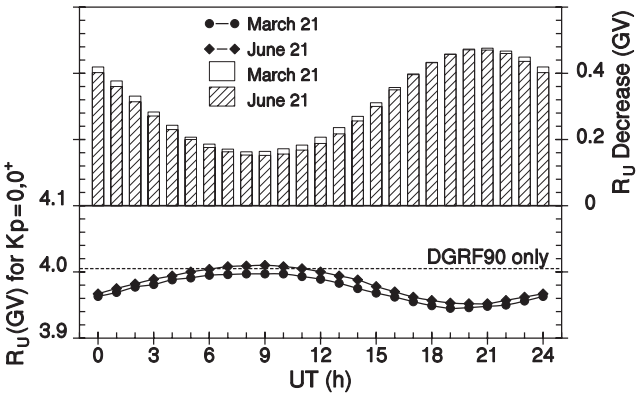


Fig. 4. – LS location (49.20° N, 20.22° E): $R_{\mathrm{U}}$ changes in the DGRF90 and Tsyg89 field models for March 21 and June 21, 1990 and $Kp = 0, 0^{+}$ (lower panel) and the corresponding $R_{\mathrm{U}}$ decrease for $Kp \geq 5^{-}$ (upper panel).

filled triangles in the upper panel of fig. 2 (2001 evaluations). From there, it is possible to confirm the slowly variable and the decreasing $R_{\mathrm{C}}$ trends for LS and LARC, respectively. Hence, we evaluated the $L$ parameter at the 20 km altitude for LS and LARC locations (http://www.spenvis.oma.be/) from 1945 to 2000 epoch (see fig. 2 for LARC, lower left panel) and we found that the $L$ change, which was $< 0.02$ for LS, resulted to be $> 0.1$ for LARC between 1965 and 1990 and the suggested test for the cut-off/$L$ relationship was performed, using the 2001 $R_{\mathrm{C}}$ evaluation. Results show that indeed cosmic-ray cut-offs follow the $L$ values and the dependence is more steeper than $L^{-2}$ for LARC location (see fig. 2, lower right panel). We remind that the origin of the cut-off and the $L$ variability is in the long-term temporal change of the geomagnetic field, which is often referred to as the *the secular variation* (*e.g.* [28] and references therein).

In the following we will concentrate our investigation on the 1990 epoch only. From the internal geomagnetic-field model we obtained: $R_{\mathrm{L}} = 3.498$ GV, $R_{\mathrm{C}} = 3.883$ GV and $R_{\mathrm{U}} = 4.005$ GV, for LS. Including the external field values (the Tsyg89 model) computations were performed for March 21, June 21, September 21 and December 21, using the following rigidity steps: $S = 0.001$ for 2.000–4.100 GV, $S = 0.01$ for 4.11–4.50 GV, $S = 0.1$ for 4.6–10.0 GV and $S = 1$ for 11–20 GV. Figure 3 shows the daily penumbra variability for March 21, 1990 in the two extreme cases of the Tsyg89 model. We observe that there exists an asymmetry in MLT (magnetic local time; for 1999 epoch the MLT midnight (MN) can be assumed as 21:47 UT, http://nssdc.gsfc.nasa.gov/space/model/), which is increasing with the $Kp$ index. Moreover, the whole pattern of the penumbra is shifted to the lower-rigidity range when the external field is perturbed. Thus, the magnetospheric transparency for cosmic rays is improving with increasing geomagnetic disturbances, especially at low rigidities, and their access becomes more sensitive to the MLT of the detector location. This is better seen in fig. 4, where the $R_{\mathrm{U}}$ variability is reported for March 21 and June 21, 1990 for $Kp = 0, 0^{+}$ (lower panel) and compared with the $R_{\mathrm{U}}$ value for DGRF90 only. For $Kp$ values greater than the one reported, the $R_{\mathrm{U}}$ is decreasing with the $Kp$ increase. The upper panel of fig. 4 shows the maximum decrease obtained, which corresponds to $Kp \geq 5^{-}$. In the same figure it is possible to check that the seasonal variation has a lower importance than the diurnal one (similar results were obtained for September 21 and December 21, in agreement with findings for

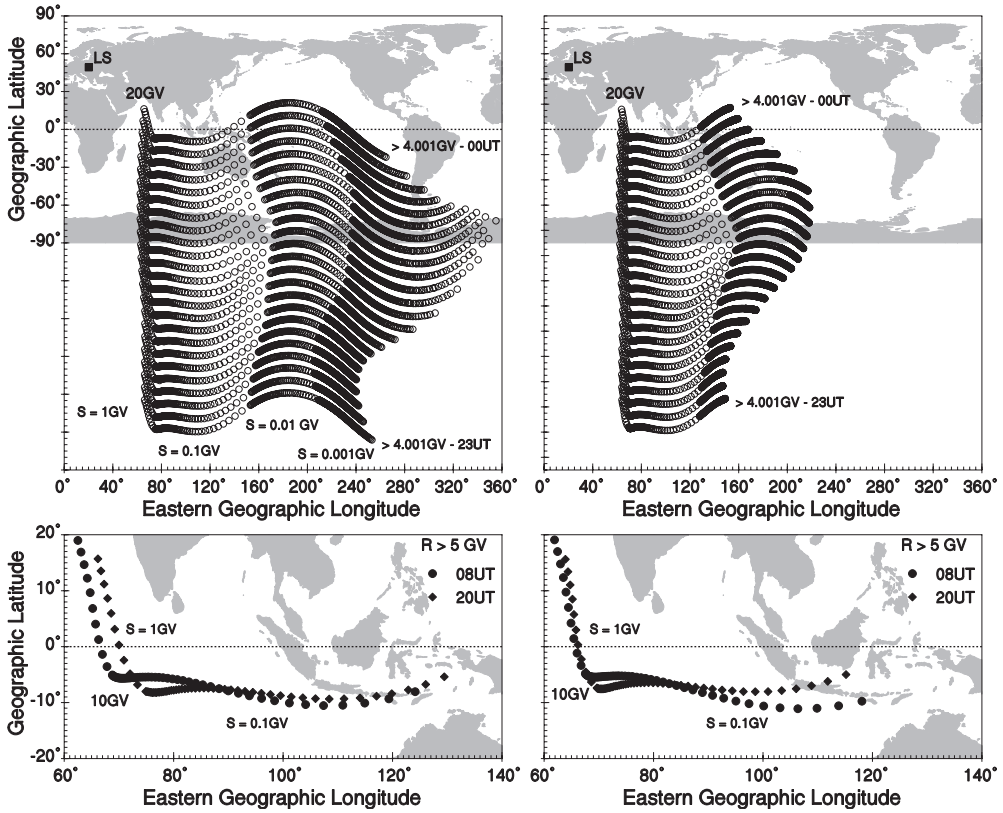


Fig. 5. – LS location (49.20° N, 20.22° E): asymptotic directions for March 21, 1990 from 00 UT (top) to 23 UT (bottom), for $Kp = 0, 0^+$ level (upper left panel) and $Kp \geq 5^-$ (upper right panel); data trends were shifted downward by $10^\circ \times h$ ($h = 0, ...23$). In the lower panels the asymptotic directions for $R > 5$ GV up to 20 GV for particles arriving at LS at 08 UT and 20 UT are shown for the same $Kp$ levels used in the upper panels.

other locations, *e.g.* [29]).

From the lower panel of fig. 4 it is also seen that the minimum transparency for LS location is expected around 8–9 UT, and the maximum at 20–22 UT. The upper panel of fig. 4, instead, gives prominence to the most sensitive MLT sector for cut-off changes (and consequent variations in the recorded CR intensity): the 18-24 UT. In other words, small changes in the geomagnetic activity level lead to changes in the counting rate of the detector which are larger during the night side sector than the ones occurring during the morning side. On the other hand, the net magnetospheric effect is indeed more complicated, due to the fact that also the particle asymptotic directions are changing simultaneously with the geomagnetic activity level (see sect. **4**).

## 4. – Asymptotic directions in a disturbed geomagnetic field

It was earlier recognized that asymptotic directions of charged particle arriving on the terrestrial ground are affected by the magnetospheric state [29-36]. However, few evaluations were performed for cosmic-ray detector locations. For the vertical direction

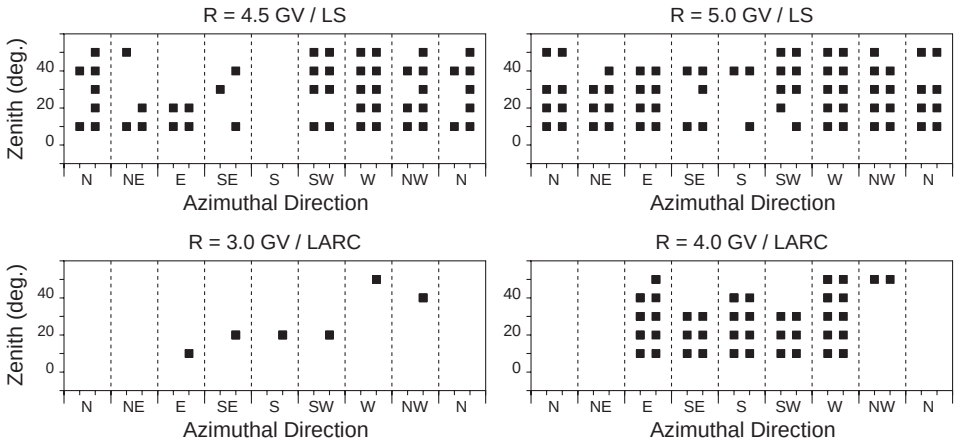


Fig. 6. – Evaluated cardinal access of charged particles at LS (top) and LARC (bottom) locations assuming $Kp = 0, 0^+$ (first column of each cardinal sector) and $Kp = 4^-, 4, 4^+$ (second column) levels for March 21, 1986. The zenith angle is changed by steps of 10° and the allowed rigidities are reported by filled boxes.

of LS the effect is illustrated in the top panels of fig. 5 for rigidities greater than 4.001 GV (*i.e.* for the ones nearly out of the penumbra region) up to 20 GV (from top to bottom in each upper panel: 00 UT, 01 UT,... 23 UT; *i.e.* shifted downward by $10° \times h$ with $h = 0, ...23$).

The above patterns indicate a clear westward shift of the asymptotic directions for the vertical particle access to the detector with the $Kp$ increase, which is particularly well pronounced for the low-rigidity part of the arriving particles. On the other hand, we remind that the threshold is lowering for increasing geomagnetic activity (as shown in fig. 4, using the daily $R_U$ variability). Also, the tendency to narrow the longitudinal extent of asymptotics with the $Kp$ increase clearly emerges, when the left and right panels of fig. 5 are compared.

The lower panels of fig. 5 illustrate, instead, the asymptotic directions for charged particles with $R > 5$ GV arriving at the LS detector only for 8 UT and 20 UT of March 21, 1990 (*i.e.* those for which the maximum differences in the $Kp$ dependence of cut-offs are expected). At 10 GV the difference is about 2.9° in latitude and 6.1° in longitude for $Kp = 0, 0^+$, and it decreases to about 2.5° and 2.1°, respectively, for $Kp \geq 5^-$. Also at 20 GV some differences, depending on the UT evaluation, remain. We should go well above 20 GV to find negligible differences between results from models with and without the external geomagnetic field.

## 5. – Particle oblique directions

In previous sections we assumed only vertically incident charged particles arriving at the detector. For particles not arriving from the zenith (which are also important for ground-based detectors, but particularly for low-altitude satellite measurements) the cut-offs and penumbra structure are differing from those related to vertically incident particles. These effects, including also the real neutron monitor response to the oblique directions, have been recently examined (see, for instance, [37, 38]).

Using a method similar to the one described by Bieber *et al.* [37] the change of the magnetospheric transparency for cosmic rays arriving obliquely at the LS and LARC detectors was also checked, using March 21, 1986 as a date for evaluation. Figure 6 gives an example of the obtained results, where it is possible to observe that the cosmic-ray transparency is improving with the $Kp$ increase ($Kp = 0, 0^+$ to $Kp = 4^-, 4, 4^+$) for the same rigidity. Considering only the geometry and adjusting the weights of the respective directions as $\cos\Theta$ ($\Theta$ being the appropriate zenith angle), the relative transparency increase resulted to be 21% at 4.5 GV for LS location. Nevertheless, this feature is decreasing with the rigidity. For 5.0 GV the net effect is only 5% at LS. This simplified estimate, however, refers to a directionally sensitive detector oriented with its normal to the zenith (such as for low-altitude satellite measurements). For the ground observatories the coupling functions, which are depending on the thickness of the atmosphere above the detector, must be considered.

## 6. – Particle trajectories affected by the residual atmosphere

The trajectory computations are usually done assuming only the particle motion in the geomagnetic field disregarding the terrestrial atmosphere. For the ground-based stations, having in mind their natural atmospheric cut-off (causing no measurable detector response to the low-energy range of primaries) this assumption is appropriate. Nevertheless, within the cosmic-ray penumbra there are complicated particle trajectories which, after a sufficiently high step number, appear to be allowed to leave the magnetosphere and which spend during their trajectory evolution some time at relatively low altitudes.

Figure 7 shows, for example, results for charged particles at 100 km altitude (70° N, 30° E), for which energy losses coming from the residual atmosphere may affect the escape from the magnetosphere or its arrival to the measurement site, due to the induced velocity variability and, hence, the conditions of the motion. To estimate the above effect we used a simplified atmospheric model (the exponential density decrease with the e-fold altitude of 8 km) and the Bethe-Bloch formula for the differential ionization losses of heavy particles ($\mathrm{d}E/\mathrm{d}x$; see the upper panel of fig. 7 for the energy/speed relationship); the obtained path length for 0.1–0.4 GV and the corresponding travel time are shown in the lower panels, while the depth of the mass penetration is reported in the upper right panel, all for $Kp \geq 5^-$ level. The summation of the energy lost was derived by using the product of the elementary trajectory length and of the differential energy loss at its central point, along the whole trajectory. In this way the total energy losses can be estimated. For $R > 0.4$ GV the energy lost is lower than 1 MeV. Hence, this effect is not relevant for ground-based detectors, since it becomes more apparent at high latitudes where the natural atmospheric cut-off (induced by the whole atmosphere) is eliminating such kind of particles. However, for low-altitude satellite measurements the estimation of the charged-particle access to the detector should include also the described effect. It is certainly worth of further study. We only show in fig. 8, as an example of the relevance of the effect, the possible change of the penumbra structure due to ionization losses at higher latitudes when ionization losses are considered for the two extreme $Kp$ levels of Tsyg89 (upper panels). If the level of 1 MeV kinetic energy is taken into account for particle energy losses the penumbra region disappears (lower panels).

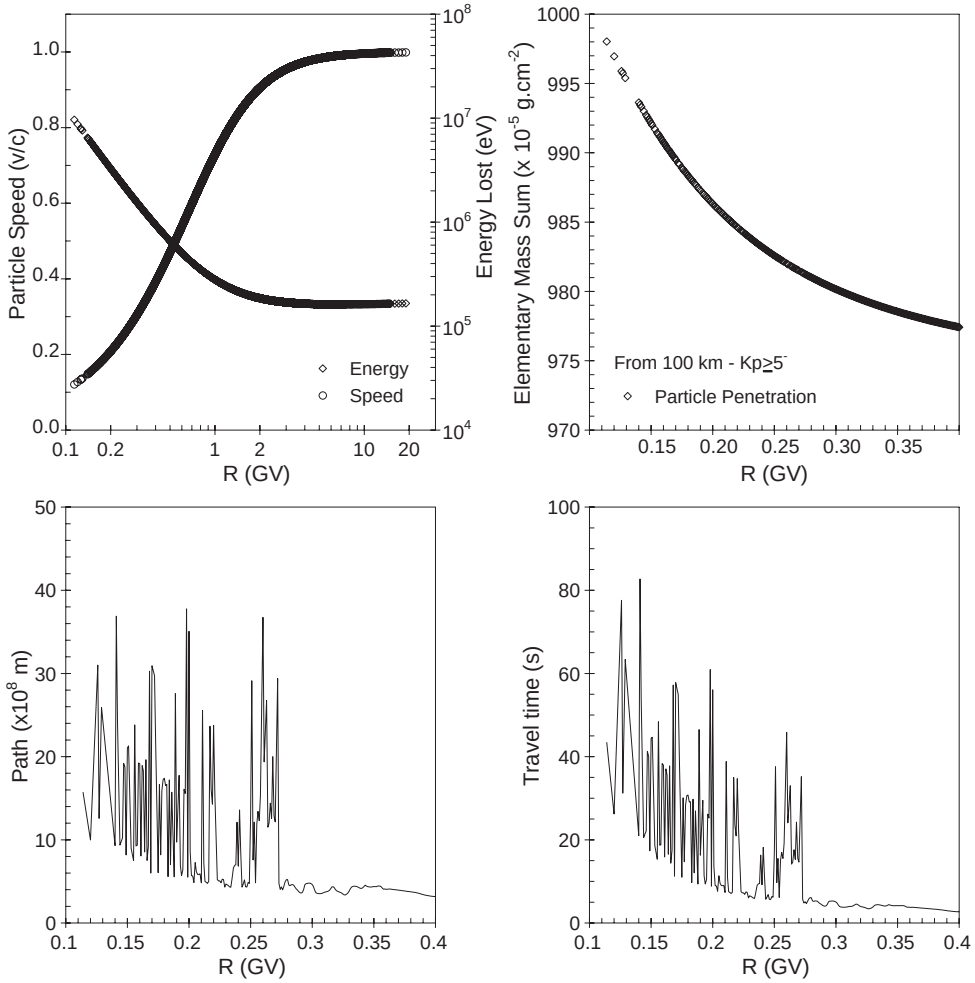


Fig. 7. – Characteristic parameters for charged particles at 100 km altitude: speed and energy losses in the residual atmosphere (upper left) for 0.1GV $< R <$ 20 GV, path length (lower left), mass penetration (upper right) and travel time (lower right) for 0.1GV $< R <$ 0.4 GV and $Kp \geq 5^-$, using the Tsyg89 model for 70° N–30° E.

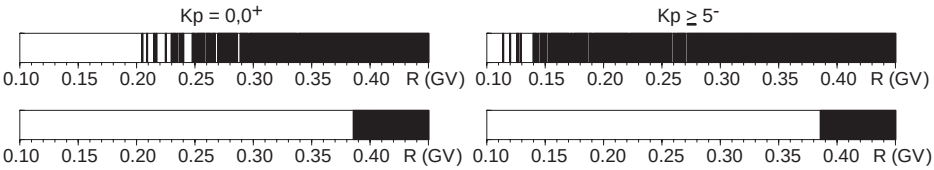


Fig. 8. – The structure of penumbra computed at the position 70° N, 30° E and 100 km a.s.l. The upper panels are obtained from trajectory computations in the Tsyg89 model with $Kp = 0, 0^+$ and $Kp \geq 5^-$, respectively. The lower panels are displaying the corresponding final structures if particles lossing at least 1 MeV of kinetic energy by ionization in the upper atmosphere are excluded.

## 7. – Conclusions

We have investigated the cosmic-ray transparency through the magnetosphere using a numerical code procedure for the solution of the equation of cosmic-ray particle motion in the geomagnetic field. It has similar properties of earlier codes using other techniques. Its application for Lomnický Štít and LARC positions shows that

i) the long-term variability of the effective rigidity cut-offs using DGRF models corresponds to the local $L$ value evolution; the time dependence of $R_{\mathrm{C}}$ is proportional to $L^{-\alpha}$, with $\alpha \sim 3$ at LARC location (fig. 2);

ii) the magnetospheric particle transparency increases with the geomagnetic activity level and there exists a significant daily variation in the terrestrial transparency (figs. 3 and 4); the largest cut-off variabilities are observed around the 20 UT and the smallest ones at 8 UT for LS;

iii) increasing the $Kp$ values the particle asymptotic directions shift westward, with a tendency to narrow the coordinate range (fig. 5);

iv) above 10 GV the influence of the external field on asymptotic coordinates is small but not negligible, as can be checked in fig. 5 for LS;

v) particle energy losses in the lower residual atmosphere for latitudes above 70° (fig. 7) may influence the structure of the cosmic-ray penumbra, irrespectively of the $Kp$ level (fig. 8); the effect may have some importance for high-inclination low-altitude energetic particle measurements.

Nowadays, space weather studies demand a refinement of cosmic-ray cut-offs and asymptotic directions. This is particularly true for the worldwide evaluation of interplanetary induced effects in the terrestrial environment. Our work is a contribution to that topic.

* * *

Work peformed inside the IEP/IFSI Collaboration for 1999-2001 and partly supported by the Antarctic Research Program of Italy (PNRA) and by VEGA grant nos. 5137 & 1147. The IFSI/CNR hospitality during the preparation of a part of the work is acknowledged by PB and KK. LS is supported by IEP/SAV, while LARC by UChile/IFSI-CNR collaboration via INACH and PNRA.

REFERENCES

[1] McCracken K. G., Rao U. R., Fowler B. C., Shea M. A. and Smart D. F., *Cosmic Rays, Annals of IQSY*, **1** (1968) 198.
[2] Shea M. A. and Smart D. F., Report AFCRL-TR-75-0177502 (1975).
[3] Shea M. A. and Smart D. F., Report AFCRL-TR-75-0177510 (1975).
[4] Flueckiger E. O., Debrunner H., Smart D. F. and Shea M.A., *Proc. 16th ICRC*, **4** (1979) 273.
[5] Bravo S., *Geofis. Intern.*, **20-2** (1981) 121.
[6] Tyasto M. I. and Danilova O. A., *Proc. 19th ICRC*, **5** (1985) 324.
[7] Smart D. F., Shea M. A. and Flueckiger E. O., *Space Sci. Rev.*, **93** (2000) 305.
[8] Storini M. and Cordaro E. G., *Nuovo Cimento C*, **20** (1997) 1027.
[9] Cordaro E. G. and Storini M., *Nuovo Cimento C*, **24** (2001) 683.
[10] Kaššovicová J. and Kudela K., preprint Dept. Space Physics-IEP/SAS (1998).
[11] Sibeck D. J., Lopez R. E. and Roelof E. C., *J. Geophys. Res.*, **96** (1991) 5489.

[12] Cooke D. J., Humble J. E., Shea M. A., Smart D. F., Lund N., Rasmussen I. L., Byrnak B., Goret P. and Petrou N., *Nuovo Cimento C*, **14** (1991) 213.
[13] Regan R. D. and Rodriguez P., *Geophys. Surveys*, **4** (1981) 255.
[14] IAGA Division I Working Group 1, *J. R. Astron. Soc.*, **85** (1986) 217
[15] Tsyganenko N. A., *Planet. Space Sci.*, **37** (1989) 5.
[16] Tsyganenko N. A., *Geomagn. Aeron.*, **27** (1987) 854.
[17] Tsyganenko N. A., *Planet. Space Sci.*, **35** (1987) 1347.
[18] Tsyganenko N. A., *Space Sci. Rev.*, **54** (1990) 75.
[19] Kudo S., Wada M., Tanskanen P. and Kodama M., *J. Geophys. Res.*, **92** (1987) 4719.
[20] Flueckiger E. O., Report AFGL-TR-82-0177 (1982).
[21] Flueckiger E. O., Smart D. F. and Shea M. A., *J. Geophys. Res.*, **88** (1983) 6961.
[22] Storini M., Shea M. A., Smart D. F. and Cordaro E. G., *Proc. 26th ICRC*, **7** (1999) 402.
[23] McIlwain C. E, *J. Geophys. Res.*, **66** (1961) 3681.
[24] Galperin Yu. I. and Zinin I. V., CADR-5 Computational Code, personal communication (2000).
[25] Shea M. A., Smart D. F. and Gentile L. C., *Phys. of the Earth and Planet. Interiors*, **48** (1987) 200.
[26] Kudela K. and Storini M., *Proc. 27th ICRC*, **10** (2001) 4103.
[27] Shea M. A. and Smart D. F., *Proc. 27th ICRC*, **10** (2001) 4063.
[28] Storini M., Bobik P. and Kudela K., *Problems with charged particle rigidities cutoffs in the Antarctic ground*, in *Italian Research on Antarctic Atmosphere*, edited by M. Colacino and G. Giovanelli (SIF Conf. Proc. 69, Bologna) 2000, pp. 229-239.
[29] Danilova O. A. and Tyasto M. I., *Proc. 24th ICRC*, **4** (1995) 1066.
[30] Flueckiger E. O., Smart D. F. and Shea M. A., *J. Geophys. Res.*, **91** (1986) 7925.
[31] Flueckiger E. O. and Kobel E., *J. Geomag. Geoelectr.*, **42** (1990) 1123.
[32] Danilova O. A., Tyasto M. I., Kananen H. and Tanskanen P., *Proc. 25th ICRC*, **2** (1997) 369.
[33] Danilova O. A., Tyasto M. I., Vashenyuk E. V., Gvozdevsky B. B., Kananen H. and Tanskanen P., *Proc. 26th ICRC*, **6** (1999) 399.
[34] Kudela K., Storini M., Bobik P. and Kaššovicová J., *Access of cosmic rays to Lomnický Štít and Rome Stations*, in *Rayos Cósmicos 98*, edited by J. Medina (Universidad de Alcalá, Alcalá) 1998, pp. 71-74.
[35] Bobik P., Storini M. and Kudela K., *The influence of magnetospheric disturbances on the charged particle access to Inuvik location*, in *What are the Prospects for Cosmic Physics in Italy?*, edited by S. Aiello and A. Blanco (SIF Conf. Proc. 68, Bologna) 2000, pp. 39-44.
[36] Bobik P., Storini M. and Kudela K., *The influence of magnetospheric disturbances on the terrestrial cosmic-ray transparency*, in *Proc. of the Conference organized on the occasion of 30th anniversary of the foundation of Faculty of Electrical Engineering and Informatics / Technical University of Košice*, edited by B. Zagyi, M. Koval'ková and J. Ziman (Technical University, Košice) 1999, pp. 178-181.
[37] Clem J. M., Bieber J. W., Duldig M., Evenson P., Hall D. and Humble J., *J. Geophys. Res.*, **102** (1997) 7925.
[38] Bieber J. W., Clem J. and Evenson P., *Proc. 25th ICRC*, **2** (1997) 389.